ISSN 0006-2979, Biochemistry (Moscow) © Pleiades Publishing, Ltd., 2024.

Computational Assessment of Carotenoids as Keap1-Nrf2 Protein–Protein Interaction Inhibitors: Implications for Antioxidant Strategies

Alessandro Medoro[1], Tassadaq Hussain Jafar[1], Fabio Sallustio[2], Giovanni Scapagnini[1], Luciano Saso[3], and Sergio Davinelli[1,a]*

[1]*Department of Medicine and Health Sciences "V. Tiberio", University of Molise, Campobasso, Italy*
[2]*Department of Precision and Regenerative Medicine and Ionian Area (DIMEPRE-J), University of Bari, Bari, Italy*
[3]*Department of Physiology and Pharmacology "Vittorio Erspamer", La Sapienza University, Rome, 00185, Italy*
[a]*e-mail: sergio.davinelli@unimol.it*

Received May 8, 2024
Revised July 21, 2024
Accepted July 23, 2024

Abstract—The Keap1-Nrf2 pathway is an essential system that maintains redox homeostasis and modulates key metabolic processes, including metabolism of amino acids to promote the synthesis of antioxidant enzymes. Inhibitors of the protein-protein interaction (PPI) between Keap1 and Nrf2 have emerged as a promising strategy for developing novel classes of antioxidant agents that selectively activate this pathway without off-target effects. Carotenoids, a large family of lipophilic isoprenoids synthesized by all photosynthetic organisms, are well-known for their antioxidant activities. However, the ability of carotenoids to inhibit the Keap1-Nrf2 PPI through the involvement of specific amino acid residues has not yet been revealed. We utilized molecular docking, molecular dynamic simulations, and pharmacokinetic prediction techniques to investigate the potential of eight oxygenated carotenoids, known as xanthophylls, to inhibit Keap1. Among the compounds investigated, fucoxanthin and astaxanthin established multiple hydrogen-bonding and hydrophobic interactions within the Kelch domain of Keap1, showing remarkable binding affinities. Furthermore, fucoxanthin and astaxanthin displayed the ability to form a stable complex with Keap1 and fit into the binding pocket of its Kelch domain. These analyses led to the identification of critical amino acid residues in the binding pocket of Keap1 which are involved in the interaction with carotenoid xanthophylls. Our analyses further revealed that fucoxanthin and astaxanthin demonstrate a favorable safety profile and possess pharmacokinetic properties consistent with acceptable drug-like characteristics. These findings lay the preliminary foundation for developing a novel class of Keap1-Nrf2 PPI inhibitors with potential applications against oxidative stress-related diseases.

DOI: 10.1134/S0006297924100031

Keywords: Keap1, Nrf2, carotenoids, xanthophylls, antioxidants

INTRODUCTION

As maintaining redox homeostasis is a continuous challenge, multicellular organisms have evolved various defense systems to mitigate the toxic effects of numerous oxidants and electrophiles to which they are exposed. A prominent aspect of oxidative stress is the induction of a cellular stress response, mediated by molecular redox switches. These switches are crucial in the activation of an extensive network of antioxidant enzymes. Accordingly, this activation counteracts the oxidative challenge, thereby preserving redox homeostasis [1, 2]. The Nrf2 (nuclear factor erythroid 2 [NF-E2]-related factor 2)-Keap1 (Kelch-like ECH-associated protein 1) pathway is one of the major regulators of oxidative and electrophilic stress response, playing a pivotal role in the maintenance of the cellular redox homeostasis. Nrf2, ubiquitously expressed across various organs, is a cap'n'collar (CNC) basic region-leucine zipper (bZIP) transcription factor.

* To whom correspondence should be addressed.

It regulates the expression levels of hundreds of genes associated with homeostatic functions and oxidative stress response. This regulation occurs through the binding of Nrf2 to a DNA enhancer region known as the antioxidant response element (ARE). Furthermore, Nrf2 is involved in amino acid metabolism, promoting the synthesis of antioxidant enzymes and increasing the availability of amino acids such as cysteine, serine, glycine, and asparagine. In humans, Nrf2 consists of 605 amino acids and includes seven distinct and highly conserved Nrf2-ECH homology (Neh) domains (Neh1–Neh7) [3-5].

Although the activity of Nrf2 is regulated by various mechanisms, including at transcriptional and epigenetic levels, its proteasomal degradation is mainly mediated by the repressor Keap1. Under basal conditions, Nrf2 protein levels remain low due to its interaction with Keap1 in the cytoplasm. This interaction involves the Neh2 domain of Nrf2, which binds to Keap1 using the DLG and ETGE motifs. This binding is essential for the ubiquitination and subsequent proteasomal degradation of Nrf2. Briefly, Keap1 recruits the Cullin 3 (Cul3)-RING-box protein 1 (RBX1) E3 ubiquitin ligase complex with subsequent ubiquitination of Nrf2 by the 26S proteasome [6]. Human Keap1 contains 627 amino acids and consists of five distinct domains: the N-terminal region (NTR), the broad complex, tramtrack and bric-a-brac (BTB) domain, the intervening region (IVR), double glycine repeats (DGR) or Kelch domain, and the C-terminal region (CTR). The BTB domain facilitates dimerization and interaction with Cul3, while the Kelch domain, binds to Neh2 of Nrf2 [7]. Moreover, Keap1 contains several highly reactive Cys residues in these domains, particularly within the IVR domain, that act as cellular redox status sensors. The most common electrophilic Nrf2 inducers trigger conformational changes in Keap1 due to modifications of its cysteine residues, disrupting the Keap1-Nrf2 protein–protein interaction (PPI) and leading to the nuclear accumulation of Nrf2. This, in turn, activates a cellular defense response against oxidative stress [8, 9]. However, since the mechanism of action of these compounds involves the covalent targeting of cysteine thiols, Nrf2 inducers may lack selectivity for Keap1, potentially affecting other cysteines within the cells and leading to unpredictable off-target side effects [10].

Currently, alternative strategies to target Nrf2 with higher selectivity have attracted increasing attention. These alternative approaches focus on developing Keap1–Nrf2 PPI inhibitors to block their interaction, thereby increasing Nrf2 activity and potentially improving the safety and efficacy of treatments for oxidative stress-related diseases. To date, several noncovalent small-molecule Keap1-Nrf2 inhibitors have been described [11]. These Keap1-Nrf2 PPI inhibitors typically bind to the Kelch domain of Keap1, targeting the sites where the ETGE and DLG motifs of Nrf2 would normally bind. The Keap1-Kelch domain, a six-bladed β-propeller structure, is divided into six subpockets (P1-P6). These subpockets accommodate different amino acid residues that interact with DLG and ETGE motifs located in the Neh2 domain of Nrf2. Therefore, the higher selectivity of Keap1-Nrf2 PPI inhibitors is determined by interactions between the DLG and ETGE motifs in the Neh2 domain of Nrf2 and the corresponding subpockets within the Keap1-Kelch domain [12, 13]. This mechanism of action selectively inhibits the binding between Keap1 and Nrf2, thereby enhancing Nrf2 activity and ensuring a more targeted modulation of the pathway.

Carotenoids, which are terpenoid-based compounds, are widely distributed in algae, fungi, bacteria, and plants. They constitute a large family of fat-soluble plant pigments known for their health-promoting effects against major chronic diseases, including diabetes, cancer, and dementia [14-16]. Carotenoids are typically classified into two groups, carotenes, and xanthophylls, based on chemical and biochemical criteria. Xanthophylls, such as fucoxanthin, astaxanthin, lutein, zeaxanthin, and canthaxanthin, which are rich in double bonds, exhibit higher antioxidant properties than carotenes [17, 18]. Several experimental studies have shown that marine-derived xanthophylls, such as astaxanthin, zeaxanthin, and lutein, can activate the Nrf2 pathway and induce the expression of antioxidant enzymes, including glutathione (GSH), heme oxygenase-1 (HO-1), and superoxide dismutase (SOD) [19-21]. However, there is limited evidence suggesting that these xanthophylls may disrupt the Keap1-Nrf2 PPI by interacting with Keap1, leading to the release and activation of Nrf2 [22]. We selected from the CHEMnetBASE – Dictionary of Marine Natural Products eight microalgal xanthophylls extensively studied for their antioxidant characteristics (astaxanthin, canthaxanthin, echinenone, fucoxanthin, lutein, neoxanthin, violaxanthin, and zeaxanthin) [23-32]. We used computational methods, including molecular docking and molecular dynamic simulations (MDS), to investigate whether these xanthophyll carotenoids might serve as potential candidates for developing selective Keap1-Nrf2 PPI inhibitors.

MATERIALS AND METHODS

3D structural retrieval and preparation of the Keap1 protein. Keap1 protein (2FLU) was retrieved from the RCSB Protein Data Bank (https://www.rcsb.org/structure/2FLU). In detail, it is the crystal structure of the Kelch domain of Keap1 bound to a 16-mer peptide from Nrf2 containing a highly conserved DxETGE motif [33]. After conducting a 3D structural retrieval,

the protein underwent preparation using UCSF Chimera software (v1.12) [34]. The retrieved structure was checked for missing residues and refined removing water molecules, additional protein chains, and ligands. To ensure protein stability, energy minimization, and geometry optimization were carried out using UCSF Chimera with 1000 steps (step size 0.02 Å) and the conjugate gradient method. The protonation of wild-type histidine was done following the AMBER ff98 method [35, 36]. Energy minimization was also performed to maintain the stability of Keap1 using the Chiron energy minimization online tool [37].

Xanthophyll carotenoids selection and structure preparation. A total of eight marine-derived xanthophyll carotenoids were selected from the CHEMnetBASE – Dictionary of Marine Natural Products (https://dmnp.chemnetbase.com/chemical/ChemicalSearch.xhtml?dswid=-7750) for the study: astaxanthin, canthaxanthin, echinenone, fucoxanthin, lutein, neoxanthin, violaxanthin, and zeaxanthin. The two-dimensional (2D) chemical structures of the compounds were searched in the PubChem database [38]. In addition, 2D chemical structures were converted into a .pdb format by Chem3D Pro, and the structural optimization was performed by UCSF Chimera software (v1.12).

Molecular docking studies. AutoDock Vina software was used for molecular docking [39]. The grid size was set at 75×75×75 Å in the X, Y, and Z axes, with a grid spacing of 0.650 Å covering Keap1 active domains. Polar hydrogen atoms were added to the Keap1 protein structure, and each docking experiment consisted of 100 runs. Default parameters for van der Waals forces, electrostatic forces, AMBER force field, and intermolecular forces were used for the ligand-protein complex. The genetic algorithm was employed as the primary search protocol. All docked complexes were analyzed, and the best-docked complex based on intermolecular interactions was visualized and analyzed using Discovery Studio.

Molecular dynamics simulations (MDS). The NAMD2 simulation software (version 2.14) was used to conduct Molecular Dynamics Simulations (MDS) of docked complexes for 120 ns in a water environment [40]. The simulations utilized the Amber ff14SB force field for proteins and a General Amber Force Field (GAFF) for ligands [41, 42]. The antechamber package generated topology and coordinate files for the ligands, while Xleap prepared the simulation system [43]. The system was solvated in a cubic box with TIP3P water molecules, and the protein was positioned within 1 nm of the box edge to adhere to the minimum image convention. Neutralization was achieved by adding 10 Na^+ ions to the system. The complexes of astaxanthin and fucoxanthin contained a total of 41363 and 41385 atoms, respectively, and were protonated at a pH of 7.4. Energy minimization was performed with the conjugate gradient method to eliminate steric clashes. The equilibration process involved settling water molecules, gradual heating, and equilibration in an NPT ensemble. The production run maintained a constant temperature of 310.15 K and pressure of 1 atm with weak coupling using a Langevin thermostat and barostat. The time step used is 0.2 fs. Bond lengths involving hydrogen atoms were constrained using the SHAKE algorithm, and Particle Mesh Ewald (PME) was employed for electrostatic interactions beyond a cutoff distance.

Prediction of drug-likeness, pharmacokinetics, and toxicity. To estimate the physicochemical properties, absorption, distribution, metabolism, excretion, toxicity (ADMET) profile, pharmacodynamic and drug-likeness parameters of all the eight xanthophyll carotenoids, the mCule server, SwissADME, AdmetSAR, Molsoft, and the ProTox-II server were used as previously described [44].

RESULTS AND DISCUSSION

Molecular docking and interaction analyses. The molecular docking studies showed the best-fitted conformational binding pose of the tested xanthophyll carotenoids (astaxanthin, canthaxanthin, echinenone, fucoxanthin, lutein, neoxanthin, violaxanthin, and zeaxanthin) within Keap1. The identified binding pocket is located in the Kelch domain of Keap1, in the shared binding region with Nrf2. This domain is a β-propeller structure composed of six blades, each consisting of a four-stranded antiparallel β-sheet connected by loops. This structure serves as the binding pocket for the Nrf2 ETGE and DLG motifs and is divided into six subpockets (P1-P6) based on interactions observed in co-crystal structures of Keap1 with these motifs. Subpockets P1 and P2 are polar, containing residues such as Ser363, Arg380, Asn382, Asn414, Arg415, Ile461, Gly462, Phe478, Arg483, and Ser508. In contrast, P4 and P5 are hydrophobic, with residues Tyr525, Gln530 in P4, and Tyr334, Tyr572, Phe577 in P5. P3, located at the center of the channel formed by small polar residues, consists of Gly509, Ser555, Ala556, Gly571, Ser602, and Gly603. Finally, P6 includes residues Asp389, Ser431, His432, Gly433, Cys434, Ile435, and His436, which interact with the DLGex peptide but not with the ETGE motif [11]. Moreover, Nrf2-ETGE-motif-containing peptides, when co-crystallized with the Keap1-Kelch domain, adopt a β-hairpin structure within the binding site. This site includes residues Asp77, Glu78, Glu79, Thr80, Gly81, and Glu82. This β-hairpin conformation is stabilized by a network of intramolecular hydrogen bonds involving the backbone atoms of residues Gln75, Asp77, Asp79, Thr80, Glu82, Leu89, and the sidechain atoms of residues Asp77 and Thr80 [33, 45].

Table 1. Binding affinities calculation of astaxanthin, canthaxanthin, echinenone, fucoxanthin, lutein, neoxanthin, violaxanthin, and zeaxanthin

Compounds	Binding Affinities (Kcal/mol)
Astaxanthin	–9.0
Canthaxanthin	–8.1
Echinenone	–8.8
Fucoxanthin	–9.5
Lutein	–8.6
Neoxanthin	–8.9
Violaxanthin	–8.5
Zeaxanthin	–7.1

The molecular docking assessments of the eight xanthophyll carotenoids revealed variations in the recorded binding energies, with the docked complex exhibiting the lowest binding energy being chosen from all the docking complexes created for each compound, as detailed in Table 1. The generated docked complexes were evaluated based on docking energy scores and the number of hydrogen bonds and hydrophobic interactions. Fucoxanthin and astaxanthin (Fig. 1) showed the lowest binding affinity scores (–9.5 to –9.0 kcal/mol, respectively), while those of canthaxanthin, echinenone, lutein, neoxanthin, violaxanthin, and zeaxanthin, were lower than –7.0 kcal/mol (ranging from –7.1 to –8.9 kcal/mol), although good values that predicted a stable binding.

All intermolecular interactions, including hydrogen bonds, and hydrophobic and electrostatic interactions, contribute to the stability of the docked complex and lower binding affinity score. In particular, hydrogen bonds and hydrophobic interactions play a significant role in ligand-receptor stability. Notably, fucoxanthin and astaxanthin, the two compounds with the lowest binding scores, were firmly bound, predominantly in a planar manner, in the Kelch domains with potential hydrogen bonding interactions, as shown in Figs. 2-3 and Table 2. In detail, in the docking complex between fucoxanthin-Keap1, Arg326, Arg415, and Arg416 were the three residues involved in hydrogen bonding. Cys368, Val370, Val418, Val420, and Val467 are involved in hydrophobic interactions, contributing to the fucoxanthin stability in the binding pocket of Keap1 (Fig. 3, Table 2). Several potential residues identified in this docking analysis are already reported as crucial for Keap1–Nrf2 interaction and the PPI inhibitors, including Arg415, Gly509, Ala556, and Gly603, suggesting, due to the peculiar structure of this molecule, interaction with polar and hydrophobic subpockets [11]. These identified key residues for the fucoxanthin–Keap1 complex also showed good overlap with 8 previously reported potential residues, including Arg415, Val465, Val512, and Ala556 [22]. In this study, Wu et al. reported that fucoxanthin, extracted from seaweeds, exhibits a neuroprotective effect by the potential inhibition of the Keap1–Nrf2 complex. Biolayer interferometry (BLI) assays showed that fucoxanthin binds to Keap1 with a potential dissociation constant (Kd) of 51.6 μM, confirming its potential as Keap1-Nrf2 PPI and inducer of Nrf2 nuclear translocation and activation of the antioxidant response element (ARE). Similar to fucoxanthin, it was observed that astaxanthin also showed a strong binding interaction with residues in the Kelch domains of Keap1, including key residues such as Arg415, Gly509, Ala556, and Gly603 (Table 2), with one hydrogen bond observed at Arg415 and three hydrophobic interactions with Val467, Val512, and Cys513 (Fig. 3). For the neoxanthin–Keap1 complex,

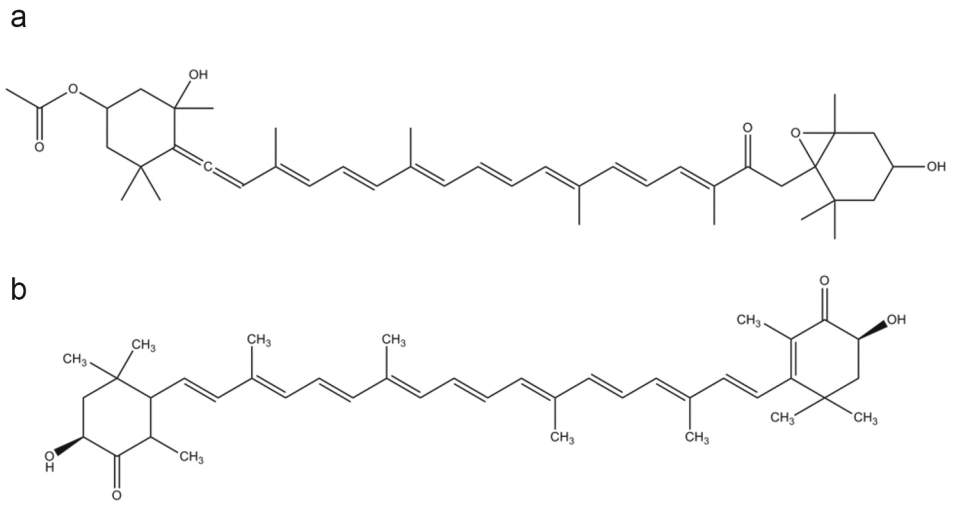

Fig. 1. 2D chemical structures of (a) fucoxanthin, and (b) astaxanthin.

Table 2. Molecular interactions of astaxanthin and fucoxanthin with Keap1

Docked complexes	Interactive residues of docking studies
Astaxanthin–Keap1	Gly364, Leu365, Ala366, Gly367, Cy368, **Arg415**, Ile416, Gly417, Val418, Gly419, Val420, Asp422, Gly423, Gly462, Val463, Gly464, Val465, Ala466, Val467, Gly509, Ala510, Gly511, Val512, Cys513, Leu557, Ile559, Gly603, Val604
Fucoxanthin–Keap1	Gly364, Leu365, Ala366, Gly367, Cys368, Val369, Val370, Gly371, Gly372, **Arg415**, **Ile416**, Gly417, Val418, Gly419, Val420, Ile421, **Asp422**, Gly423, Val463, Gly464, Val467, Gly509, Ala510, Gly511, Ala556, Leu557, Gly558, Ile559, Gly603, Val604, Gly605

Note. Bold residues indicate residues that are involved in potential hydrogen bonding.

a unique hydrogen bond with the residue Ile416 was identified. No hydrogen bonding interactions were reported in the docking complexes of canthaxanthin–Keap1, echinenone–Keap1, lutein–Keap1, violaxanthin–Keap1, and zeaxanthin–Keap1, although in the docking complex of echinenone–Keap1 some hydrophobic interactions were detected (Fig. S1 in the Online Resource 1).

Moreover, studied carotenoids may bind many Keap1 residues shared with Nrf2, including Arg415, Gly509, Ala556, and Gly603, which are all residues located in P1-P3 subpockets. Overall, these data may offer further interpretation of the antioxidant activity of xanthophyll carotenoids. Carotenoids are known to be efficient antioxidants that directly scavenge singlet molecular oxygen and peroxyl radicals, contributing to the antioxidant defense system [46]. However, there is multiple experimental evidence that xanthophyll carotenoids, particularly fucoxanthin, and astaxanthin, may inhibit Nrf2 degradation and increase Nrf2-dependent activity [20, 47-49]. Overall, our findings provide evidence for a new potential mechanism by which carotenoids may exert their antioxidant activity through the Nrf2 pathway. Among the carotenoids analyzed in this study, astaxanthin and fucoxanthin demonstrated potentially higher binding stability with Keap1, as indicated by their binding energies and the greater number of identified hydrogen bonds and hydrophobic interactions.

MDS studies. To gain further insights into the study of the interaction of the two most potential xanthophyll carotenoids, fucoxanthin and astaxanthin, with Keap1, MDS studies were performed. MDS is a method for analyzing the physical movements of atoms and molecules, providing information on conformational changes in docking complexes. As expected, some differences in docking interactions of protein-ligand complexes between AutoDock Vina and MDS analyses were detected, considering that MDS offers a dynamic view of the protein-ligand complex,

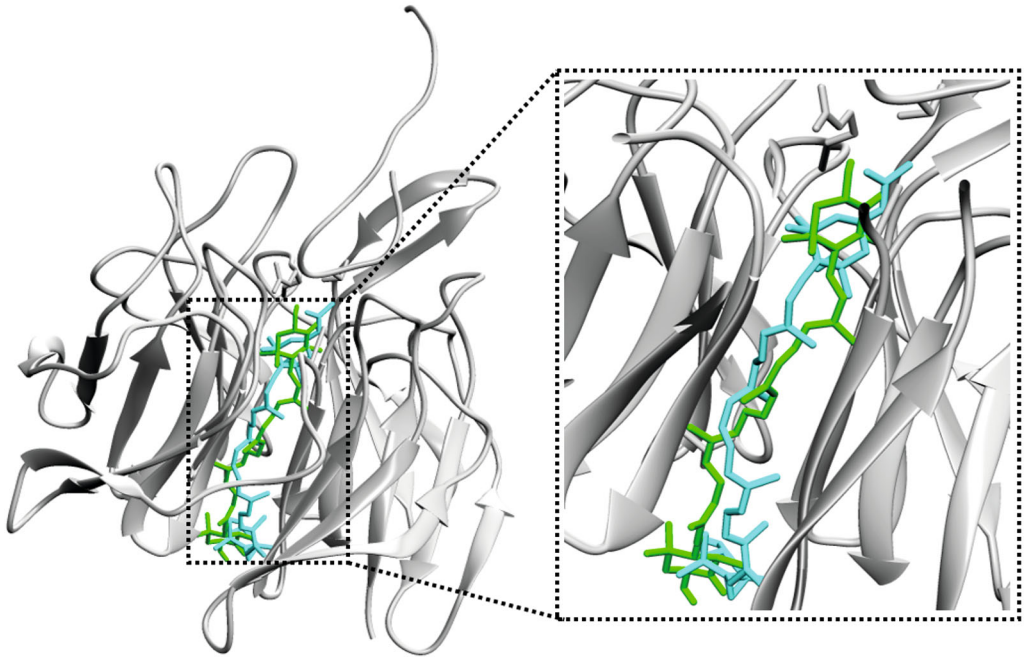

Fig. 2. 3D molecular representation of fucoxanthin (green) and astaxanthin (cyan) docking complexes with Keap1.

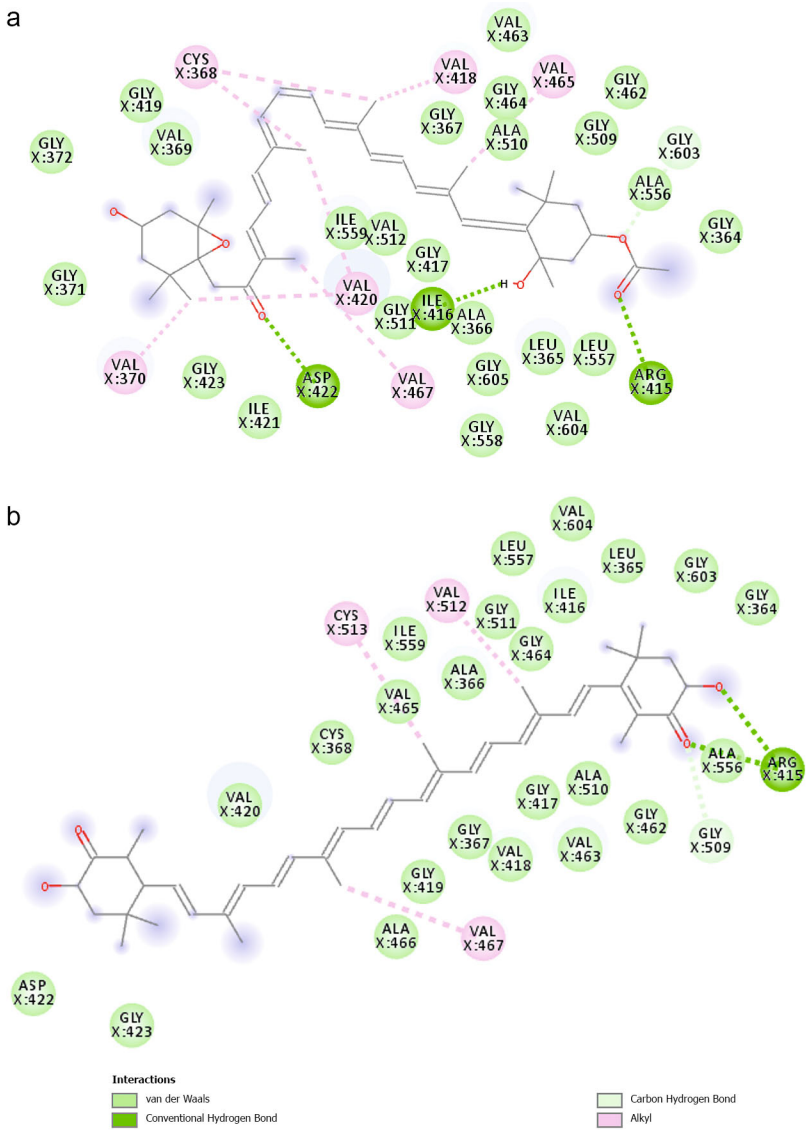

Fig. 3. 2D molecular interaction analyses of (a) fucoxanthin, and (b) astaxanthin with Keap1.

as well as revealed comprehensive and more realistic molecular interactions during the simulation system (Fig. S2 in the Online Resource 1). Overall, fucoxanthin and astaxanthin showed significant potential in the binding of the Kelch domains of Keap1, generating a very stable and tight-docked complex, as shown by the data below.

Root Mean Square Deviation (RMSD) is a measure used to quantify the structural analysis of the docking complex. In Fig. 4 RMSD values indicated the average deviation for both ligands (astaxanthin and fucoxanthin) and protein. Both fucoxanthin and astaxanthin simulation complexes with Keap1 showed that the structure remained stable throughout the simulation time with some fluctuation within the range of ~1 Å, which is an expected behavior. Therefore, the RMSD values (1.54 ± 0.08 Å in complex with astaxanthin and 1.67 ± 0.14 Å with fucoxanthin) indicate that the Keap1 underwent small local conformational changes with apparently no change in its folding and stability (Fig. 4a). Astaxanthin and fucoxanthin showed high RMSD values (2.44 ± 0.47 Å and 3.39 ± 0.35 Å, respectively), suggesting conformational changes. Fucoxanthin exhibited higher variation in ligand conformation, as indicated by its higher RMSD value, and suggests at least two different clusters for ligand conformations. The ligand's RMSD plot immediately reached a plateau, indicating stability in conformation. Astaxanthin at least exhibited two ensembles of ligands during simulation, which transformed into each other back and forth (Fig. 4b).

In addition, Root Mean Square Fluctuation (RMSF) was used to estimate the binding orientations of the ligands and structural alternations of the residues that linked to targeted protein at a specific temperature and pressure. Fluctuations in the protein residues

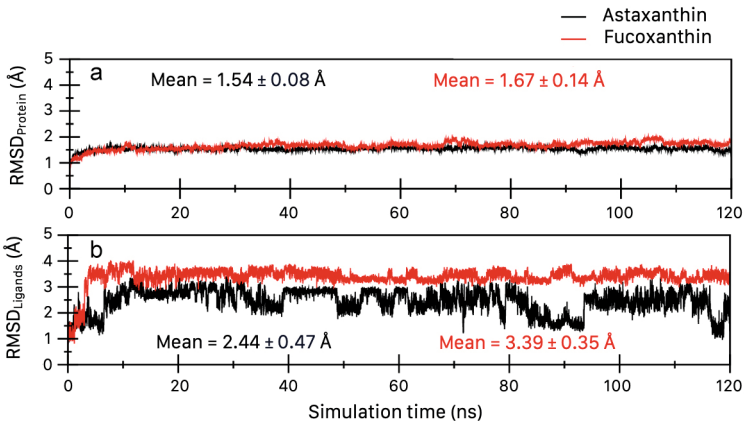

Fig. 4. a, b) RMSD detailed calculation analyses of astaxanthin (black line), and fucoxanthin (red line) complexes with Keap1 during 120 ns MDS.

of Keap1 and both changes in the ligand atom position of astaxanthin and fucoxanthin were calculated from the 120 ns trajectory. These RMSF studies endorsed that both complexes in our simulations exhibited ≤2.0 Å protein RMSF values indicating firmly bound ligands with great protein stability and rigidity in the structures (Fig. S3A in the Online Resource 1).

Both complexes showed a very stable radius of gyration with a fluctuation of 1 Å, which indicates the stability and the compactness of the 3D protein structure. The slight fluctuation within the 1 Å radius-of-gyration value during the MDS time indicated a slight opening and closing of the N- and C-terminal domains (Fig. S3B in the Online Resource 1). Notably, these were very small fluctuations in the normal range of radius-of-gyration, which indicates that the protein–ligand system remains compact during molecular dynamics simulation and that no unfolding event is observed. In detail, the radius of gyration of astaxanthin and fucoxanthin indicated no change in the protein compactness, remaining highly compact with consistent values and smaller standard deviations (18.09 ± 0.07 Å and 18.06 ± 0.06 Å, respectively).

To deepen the molecular interactions between Keap1 active site residues and astaxanthin and fucoxanthin, the free energy of the docked complexes was calculated using the MM/GBSA method. Molecular interactions between Keap1 binding sites residues and astaxanthin, and fucoxanthin after every 1 ns (120 frames in total) portrayed highly favorable electrostatic energies, and polar solvation-free energies, and showed that van der Waals forces were highly favorable interactions contributing to the stability of the molecular docking systems (Fig. 5). The overall least binding energies obtained for astaxanthin (–46.84 ± 7.39 kcal/mol) and fucoxanthin (–52.66 ± 4.77 kcal/mol) docking com-

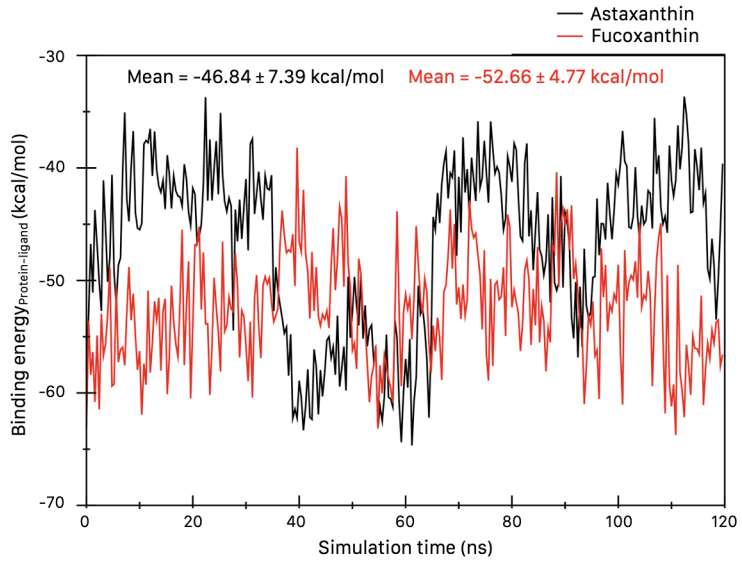

Fig. 5. MM/GBSA protein–ligand binding energy calculated for astaxanthin (black line), and fucoxanthin (red line) after every 1 ns (120 frames in total).

Table 3. Drug-likeness analyses of astaxanthin, canthaxanthin, echinenone, fucoxanthin, lutein, neoxanthin, violaxanthin, and zeaxanthin

Compounds	RO5	Veber Rule	Drug-likeness	Bioavailability
Astaxanthin	no	yes	–0.13	0.17
Canthaxanthin	no	yes	0.08	0.17
Echinenone	no	yes	0.19	0.17
Fucoxanthin	no	no	–0.35	0.17
Lutein	no	yes	–0.33	0.17
Neoxanthin	no	yes	–0.78	0.17
Violaxanthin	no	yes	–1.49	0.17
Zeaxanthin	no	yes	–0.18	0.17

plexes represented binding flexibility. Although these findings showed that both ligands remained in bound form throughout the simulation time with very good binding energy, fucoxanthin may bind with slightly more favorable energy to Keap1 with respect to astaxanthin. Moreover, ligand-protein hydrogen bonds play a significant role in determining the binding efficacy of a ligand on the binding pockets of the protein. The total number of hydrogen bonds formed between ligand and protein is shown in Fig. S4 in the Online Resource 1. Astaxanthin and fucoxanthin, during 120 ns simulation time, maintained almost two hydrogen bonds formed at the interface of protein at most points of the simulation time.

Drug-likeness, pharmacokinetics, and toxicity analyses. All compounds investigated in this study were subjected to drug-likeness, pharmacodynamic, and toxicity profiling to assess their potential safety, with overall very good results for all the xanthophylls tested. Table S1 in the Online Resource 1 shows the cheminformatics analysis of the compounds. The molecular weight (g/mol) of all compounds was also comparable with the standard value (<5000 g/mol). The SwissADME analyses presented in Table 3 show that all the analyzed carotenoids have more than one violation in RO5, the five rule-based filters allow prediction of whether a molecule is defined as an orally active drug. However, as shown in Table 3 and Table S1 in the Online Resource 1, these carotenoids, except fucoxanthin, met the requirements of drug-likeness of Veber filters. Moreover, also drug-likeness scores of all the compounds calculated using MolSoft and synthetic bioavailability scores calculated by SwissADME were in contrast to the RO5 results. Fucoxanthin and astaxanthin displayed good drug-likeness scores (–0.35 and –0.13) and bioavailability scores within the range of >10%. All the drug-likeness scores of the other carotenoids were comprised between 0.08 and –1.49 (Table 3 and Table S1 in the Online Resource 1).

All compounds were predicted to be absorbed by the human intestine and displayed promising results for the blood brain barrier (BBB) permeability. Moreover, non-toxic and non-carcinogenic behaviors were observed for all the xanthophyll carotenoids. According to the predicted results, overall, these compounds showed lower toxicity (hepatotoxicity, immunotoxicity, mutagenicity, and cytotoxicity), and carcinogenicity. The overall predicted results justified their good ADMET behavior (Table S2 in the Online Resource 1). According to the predicted ADMET analysis, some of the compounds had a very high lethal dose 50 (LD_{50}), such as astaxanthin (4600 mg/kg), canthaxanthin (10,000 mg/kg), and echinenone (10,000 mg/kg), which were classified as non-toxic for acute oral toxicity. On the other side, because of their lower LD_{50}, fucoxanthin (130 mg/kg), lutein (10 mg/kg), neoxanthin (50 mg/kg), violaxanthin (55 mg/kg), and zeaxanthin (not available) were classified as harmful if swallowed ($50 < LD_{50} \leq 300$) or fatal if swallowed ($5 < LD_{50} \leq 50$). In the toxicity analyses, astaxanthin confirmed its non-toxic potential, showing no hepatotoxicity, carcinogenicity, mutagenicity, or cytotoxicity. On the other hand, fucoxanthin showed carcinogenicity and immunotoxicity potential with more probability.

In addition, all compounds were screened with ProTox-II to predict whether they could interfere with various biological pathways. The results revealed that fucoxanthin and astaxanthin were inactive against all the targeted biological pathways. In detail, astaxanthin, echinenone, fucoxanthin, neoxanthin, and violaxanthin showed no potential activity against nuclear receptor pathways and stress response pathways, including aryl hydrocarbon receptor (Ahr), androgen receptor (AR), androgen receptor ligand binding

domain (AR-LBD), estrogen receptor alpha (ER), Estrogen receptor ligand binding domain (ER-LBD), peroxisome proliferator-activated receptor gamma (PPAR-γ), and p53. Canthaxanthin could interfere with ER and ER-LBD, and lutein and zeaxanthin with p53 (Table S3 in the Online Resource 1).

CONCLUSIONS

Keap1, a highly redox-sensitive member of the BTB-Kelch substrate adaptor protein family, is known to mediate the ubiquitination of Nrf2, a master regulator of the antioxidant response. This study employs a computational approach to explore the potential of oxygenated carotenoids, known as xanthophylls, as candidates for inhibiting the Keap1-Nrf2 PPI. Recently, inhibitors of the Keap1-Nrf2 PPI have gained increasing attention as a means to selectively target Nrf2 without off-target effects, leading to the development of novel classes of potential preventive and therapeutic agents for a variety of diseases characterized by oxidative stress. Although the reliability of *in silico* predictions greatly depends on the accuracy of molecular docking simulations and scoring functions, computational techniques remain crucial for accelerating the screening of Keap1-Nrf2 PPI inhibitors and diversifying their chemical scaffolds. In this study, three-dimensional structural information, molecular docking screening, and interaction analysis revealed the structural determinants underpinning the binding process between carotenoid xanthophylls, especially fucoxanthin and astaxanthin, and Keap1. These analyses led to the identification of critical amino acid residues in the binding pocket of Keap1 which are involved in the interaction with carotenoid xanthophylls. However, fucoxanthin and astaxanthin exhibited a stronger binding interaction with residues in the Kelch domains of Keap1 than other carotenoid xanthophylls. We then performed MDS studies to elucidate the dynamic behavior and stability of the interactions between fucoxanthin, astaxanthin, and Keap1. Through a 120 ns simulation trajectory, the results offered insights into the temporal evolution of protein–ligand complexes, deciphering the forces underlying their associations. Notably, fucoxanthin and astaxanthin formed a highly stable and tightly docked complex throughout the simulation period, establishing multiple hydrogen bonds with Keap1 and characterized by very good binding energy. Moreover, favorable pharmacokinetic and safety profiles have demonstrated the drug-like properties of these compounds, enhancing their potential as Keap1-Nrf2 PPI inhibitors. Overall, this study provides theoretical support that could stimulate further research into antioxidant strategies involving carotenoid xanthophylls, particularly focusing on their potential to inhibit the Keap1-Nrf2 PPI in experimental models of oxidative stress.

Supplementary information. The online version contains supplementary material available at https://doi.org/10.1134/S0006297924100031.

Contributions. Conceptualization, A.M., S.D., and G.S.; methodology, A.M. and S.D.; formal analysis, A.M. and T.H.J.; writing – original draft preparation, A.M., T.H.J., and F.S.; writing – review and editing, G.S., L.S., and S.D.

Funding. This work was supported by ongoing institutional funding. No additional grants to carry out or direct this particular research were obtained.

Ethics declarations. This work does not contain any studies involving human and animal subjects. The authors of this work declare that they have no conflicts of interest.

REFERENCES

1. Go, Y. M., and Jones, D. P. (2013) The redox proteome, *J. Biol. Chem.*, **288**, 26512, https://doi.org/10.1074/jbc.r113.464131.
2. Brigelius-Flohé, R., and Flohé, L. (2011) Basic principles and emerging concepts in the redox control of transcription factors, *Antioxid. Redox Signal.*, **15**, 2335-2381, https://doi.org/10.1089/ars.2010.3534.
3. Hybertson, B. M., Gao, B., Bose, S. K., and McCord, J. M. (2011) Oxidative stress in health and disease: the therapeutic potential of Nrf2 activation, *Mol. Aspects Med.*, **32**, 234-246, https://doi.org/10.1016/j.mam.2011.10.006.
4. Medoro, A., Saso, L., Scapagnini, G., and Davinelli, S. (2023) NRF2 signaling pathway and telomere length in aging and age-related diseases, *Mol. Cell. Biochem.*, https://doi.org/10.1007/s11010-023-04878-x.
5. Malhotra, D., Portales-Casamar, E., Singh, A., Srivastava, S., Arenillas, D., Happel, C., Shyr, C., Wakabayashi, N., Kensler, T. W., Wasserman, W. W., and Biswal, S. (2010) Global mapping of binding sites for Nrf2 identifies novel targets in cell survival response through chip-seq profiling and network analysis, *Nucleic Acids Res.*, **38**, 5718-5734, https://doi.org/10.1093/nar/gkq212.
6. Baird, L., and Yamamoto, M. (2020) The molecular mechanisms regulating the KEAP1-NRF2 pathway, *Mol. Cell. Biol.*, **40**, e00099-20, https://doi.org/10.1128/mcb.00099-20.
7. Canning, P., Sorrell, F. J., and Bullock, A. N. (2015) Structural basis of Keap1 interactions with Nrf2, *Free Radic. Biol. Med.*, **88**, 101-107, https://doi.org/10.1016/j.freeradbiomed.2015.05.034.
8. Davinelli, S., Medoro, A., Intrieri, M., Saso, L., Scapagnini, G., and Kang, J. X. (2022) Targeting NRF2-KEAP1 axis by Omega-3 fatty acids and their derivatives:

emerging opportunities against aging and diseases, *Free Radic. Biol. Med.*, **193**, 736-750, https://doi.org/10.1016/j.freeradbiomed.2022.11.017.

9. Dayalan Naidu, S., and Dinkova-Kostova, A. T. (2020) KEAP1, a cysteine-based sensor and a drug target for the prevention and treatment of chronic disease, *Open Biol.*, **10**, 200105, https://doi.org/10.1098/rsob.200105.
10. Lee, S., and Hu, L. (2020) Nrf2 activation through the inhibition of Keap1-Nrf2 protein-protein interaction, *Med. Chem. Res.*, **29**, 846-867, https://doi.org/10.1007/s00044-020-02539-y.
11. Crisman, E., Duarte, P., Dauden, E., Cuadrado, A., Rodríguez-Franco, M. I., López, M. G., and León, R. (2023) KEAP1-NRF2 protein-protein interaction inhibitors: design, pharmacological properties and therapeutic potential, *Med. Res. Rev.*, **43**, 237-287, https://doi.org/10.1002/med.21925.
12. Pallesen, J. S., Tran, K. T., and Bach, A. (2018) Non-covalent small-molecule Kelch-like ECH-associated protein 1-nuclear factor erythroid 2-related Factor 2 (Keap1-Nrf2) Inhibitors and their potential for targeting central nervous system diseases, *J. Med. Chem.*, **61**, 8088-8103, https://doi.org/10.1021/acs.jmedchem.8b00358.
13. Leung, C. H., Zhang, J. T., Yang, G. J., Liu, H., Han, Q. B., and Ma, D. L. (2019) Emerging screening approaches in the development of Nrf2-Keap1 protein-protein interaction inhibitors, *Int. J. Mol. Sci.*, **20**, 4445, https://doi.org/10.3390/ijms20184445.
14. Davinelli, S., Ali, S., Solfrizzi, V., Scapagnini, G., and Corbi, G. (2021) Carotenoids and cognitive outcomes: a meta-analysis of randomized intervention trials, *Antioxidants*, **10**, 223, https://doi.org/10.3390/antiox10020223.
15. Saini, R. K., Keum, Y. S., Daglia, M., and Rengasamy, K. R. (2020) Dietary carotenoids in cancer chemoprevention and chemotherapy: a review of emerging evidence, *Pharmacol. Res.*, **157**, 104830, https://doi.org/10.1016/j.phrs.2020.104830.
16. Medoro, A., Intrieri, M., Passarella, D., Willcox, D. C., Davinelli, S., and Scapagnini, G. (2024) Astaxanthin as a metabolic regulator of glucose and lipid homeostasis, *J. Funct. Foods*, **112**, 105937, https://doi.org/10.1016/j.jff.2023.105937.
17. Thomas, S. E., and Johnson, E. J. (2018) Xanthophylls, *Adv. Nutr.*, **9**, 160, https://doi.org/10.1093/advances/nmx005.
18. Pereira, A. G., Otero, P., Echave, J., Carreira-Casais, A., Chamorro, F., Collazo, N., Jaboui, A., Lourenço-Lopes, C., Simal-Gandara, J., and Prieto, M. A. (2021) Xanthophylls from the sea: algae as source of bioactive carotenoids, *Mar. Drugs*, **19**, 188, https://doi.org/10.3390/md19040188.
19. Davinelli, S., Saso, L., D'angeli, F., Calabrese, V., Intrieri, M., and Scapagnini, G. (2022) Astaxanthin as a modulator of Nrf2, NF-κB, and their crosstalk: molecular mechanisms and possible clinical applications, *Molecules*, **27**, 502, https://doi.org/10.3390/molecules27020502.
20. Zou, X., Gao, J., Zheng, Y., Wang, X., Chen, C., Cao, K., Xu, J., Li, Y., Lu, W., Liu, J., and Feng, Z. (2014) Zeaxanthin induces Nrf2-mediated phase II enzymes in protection of cell death, *Cell Death Dis.*, **55**, e1218, https://doi.org/10.1038/cddis.2014.190.
21. Chang, J., Zhang, Y., Li, Y., Lu, K., Shen, Y., Guo, Y., Qi, Q., Wang, M., and Zhang, S. (2018) NrF2/ARE and NF-κB pathway regulation may be the mechanism for lutein inhibition of human breast cancer cell, *Futur. Oncol.*, **14**, 719-726, https://doi.org/10.2217/fon-2017-0584.
22. Wu, W., Han, H., Liu, J., Tang, M., Wu, X., Cao, X., Zhao, T., Lu, Y., Niu, T., Chen, J., and Chen, H. (2021) Fucoxanthin prevents 6-OHDA-induced neurotoxicity by targeting Keap1, *Oxid. Med. Cell. Longev.*, **2021**, 6688708, https://doi.org/10.1155/2021/6688708.
23. Ahmed, F., Fanning, K., Netzel, M., and Schenk, P. M. (2015) Induced carotenoid accumulation in *Dunaliella salina* and *Tetraselmis suecica* by plant hormones and UV-C radiation, *Appl. Microbiol. Biotechnol.*, **99**, 9407-9416, https://doi.org/10.1007/s00253-015-6792-x.
24. Pasquet, V., Morisset, P., Ihammouine, S., Chepied, A., Aumailley, L., Berard, J. B., Serive, B., Kaas, R., Lanneluc, I., Thiery, V., Lafferriere, M., Piot, J. M., Patrice, T., Cadoret, J. P., and Picot, L. (2011) Antiproliferative activity of violaxanthin isolated from bioguided fractionation of *Dunaliella tertiolecta* extracts, *Mar. Drugs*, **9**, 819-831, https://doi.org/10.3390/md9050819.
25. Abe, K., Hattori, H., and Hirano, M. (2007) Accumulation and antioxidant activity of secondary carotenoids in the aerial microalga *Coelastrella striolata* var. multistriata, *Food Chem.*, **100**, 656-661, https://doi.org/10.1016/j.foodchem.2005.10.026.
26. Xia, S., Wang, K., Wan, L., Li, A., Hu, Q., and Zhang, C. (2013) Production, characterization, and antioxidant activity of fucoxanthin from the marine diatom *Odontella aurita*, *Mar. Drugs*, **11**, 2667-2681, https://doi.org/10.3390/md11072667.
27. Přibyl, P., Pilný, J., Cepák, V., and Kaštánek, P. (2016) The role of light and nitrogen in growth and carotenoid accumulation in *Scenedesmus* sp., *Algal Res.*, **16**, 69-75, https://doi.org/10.1016/j.algal.2016.02.028.
28. Neumann, U., Derwenskus, F., Flister, V. F., Schmid-Staiger, U., Hirth, T., and Bischoff, S. C. (2019) Fucoxanthin, A carotenoid derived from phaeodactylum tricornutum exerts antiproliferative and antioxidant activities *in vitro*, *Antioxidants*, **8**, 183, https://doi.org/10.3390/antiox8060183.
29. Medoro, A., Davinelli, S., Milella, L., Willcox, B. J., Allsopp, R. C., Scapagnini, G., and Willcox, D. C. (2023) Dietary astaxanthin: a promising antioxidant and anti-inflammatory agent for brain aging

and adult neurogenesis, *Mar. Drugs*, **21**, 643, https://doi.org/10.3390/md21120643.

30. Terao, J. (2023) Revisiting carotenoids as dietary antioxidants for human health and disease prevention, *Food Funct.*, **14**, 7799-7824, https://doi.org/10.1039/d3fo02330c.
31. Srivastava, R. (2021) Physicochemical, antioxidant properties of carotenoids and its optoelectronic and interaction studies with chlorophyll pigments, *Sci. Rep.*, **11**, 18365, https://doi.org/10.1038/s41598-021-97747-w.
32. Miller, N. J., Sampson, J., Candeias, L. P., Bramley, P. M., and Rice-Evans, C. A. (1996) Antioxidant activities of carotenes and xanthophylls, *FEBS Lett.*, **384**, 240-242, https://doi.org/10.1016/0014-5793(96)00323-7.
33. Lo, S. C., Li, X., Henzl, M. T., Beamer, L. J., and Hannink, M. (2006) Structure of the Keap1:Nrf2 interface provides mechanistic insight into Nrf2 signaling, *EMBO J.*, **25**, 3605-3617, https://doi.org/10.1038/sj.emboj.7601243.
34. Pettersen, E. F., Goddard, T. D., Huang, C. C., Couch, G. S., Greenblatt, D. M., Meng, E. C., and Ferrin, T. E. (2004) UCSF Chimera – a visualization system for exploratory research and analysis, *J. Comput. Chem.*, **25**, 1605-1612, https://doi.org/10.1002/jcc.20084.
35. Huang, Z., Lin, Z., and Song, C. (2007) Protonation processes and electronic spectra of histidine and related ions, *J. Phys. Chem. A*, **111**, 4340-4352, https://doi.org/10.1021/jp067280a.
36. Uranga, J., Mikulskis, P., Genheden, S., and Ryde, U. (2012) Can the protonation state of histidine residues be determined from molecular dynamics simulations? *Comput. Theor. Chem.*, **1000**, 75-84, https://doi.org/10.1016/j.comptc.2012.09.025.
37. Ramachandran, S., Kota, P., Ding, F., and Dokholyan, N. V. (2011) Automated minimization of steric clashes in protein structures, *Proteins*, **79**, 261-270, https://doi.org/10.1002/prot.22879.
38. Kim, S., Thiessen, P. A., Bolton, E. E., Chen, J., Fu, G., Gindulyte, A., Han, L., He, J., He, S., Shoemaker, B. A., Wang, J., Yu, B., Zhang, J., and Bryant, S. H. (2016) PubChem substance and compound databases, *Nucleic Acids Res.*, **44**, D1202-D1213, https://doi.org/10.1093/nar/gkv951.
39. Trott, O., and Olson, A. J. (2010) AutoDock Vina: improving the speed and accuracy of docking with a new scoring function, efficient optimization and multithreading, *J. Comput. Chem.*, **31**, 455, https://doi.org/10.1002/jcc.21334.
40. Phillips, J. C., Braun, R., Wang, W., Gumbart, J., Tajkhorshid, E., Villa, E., Chipot, C., Skeel, R. D., Kalé, L., and Schulten, K. (2005) Scalable molecular dynamics with NAMD, *J. Comput. Chem.*, **26**, 1781-1802, https://doi.org/10.1002/jcc.20289.
41. Wang, J., Wolf, R. M., Caldwell, J. W., Kollman, P. A., and Case, D. A. (2004) Development and testing of a general amber force field, *J. Comput. Chem.*, **25**, 1157-1174, https://doi.org/10.1002/jcc.20035.
42. Maier, J. A., Martinez, C., Kasavajhala, K., Wickstrom, L., Hauser, K. E., and Simmerling, C. (2015) ff14SB: improving the accuracy of protein side chain and backbone parameters from ff99SB, *J. Chem. Theory Comput.*, **11**, 3696-3713, https://doi.org/10.1021/acs.jctc.5b00255.
43. Yu, Y., Xu, S., He, R., and Liang, G. (2023) Application of molecular simulation methods in food science: status and prospects, *J. Agric. Food Chem.*, **71**, 2684-2703, https://doi.org/10.1021/acs.jafc.2c06789.
44. Medoro, A., Jafar, T. H., Ali, S., Trung, T. T., Sorrenti, V., Intrieri, M., Scapagnini, G., and Davinelli, S. (2023) *In silico* evaluation of geroprotective phytochemicals as potential sirtuin 1 interactors, *Biomed. Pharmacother.*, **161**, 114425, https://doi.org/10.1016/j.biopha.2023.114425.
45. Padmanabhan, B., Tong, K. I., Ohta, T., Nakamura, Y., Scharlock, M., Ohtsuji, M., Kang, M. I., Kobayashi, A., Yokoyama, S., and Yamamoto, M. (2006) Structural basis for defects of Keap1 activity provoked by its point mutations in lung cancer, *Mol. Cell*, **21**, 689-700, https://doi.org/10.1016/j.molcel.2006.01.013.
46. Stahl, W., and Sies, H. (2023) Antioxidant activity of carotenoids, *Mol. Aspects Med.*, **24**, 345-351, https://doi.org/10.1016/s0098-2997(03)00030-x.
47. Roselli, S., Pundavela, J., Demont, Y., Faulkner, S., Keene, S., Attia, J., Jiang, C. C., Zhang, X. D., Walker, M. M., and Hondermarck, H. (2015) Sortilin is associated with breast cancer aggressiveness and contributes to tumor cell adhesion and invasion, *Oncotarget*, **6**, 10473-10486, https://doi.org/10.18632/oncotarget.3401.
48. Frede, K., Ebert, F., Kipp, A. P., Schwerdtle, T., and Baldermann, S. (2017) Lutein activates the transcription factor Nrf2 in human retinal pigment epithelial cells, *J. Agric. Food Chem.*, **65**, 5944-5952, https://doi.org/10.1021/acs.jafc.7b01929.
49. Li, Z., Dong, X., Liu, H., Chen, X., Shi, H., Fan, Y., Hou, D., and Zhang, X. (2013) Astaxanthin protects ARPE-19 cells from oxidative stress via upregulation of Nrf2-regulated phase II enzymes through activation of PI3K/Akt, *Mol. Vis.*, **19**, 1656.